Geosci. Model Dev. Discuss., 5, 1203–1227, 2012
www.geosci-model-dev-discuss.net/5/1203/2012/
doi:10.5194/gmdd-5-1203-2012

Geoscientific Model Development Discussions

Pre-industrial and mid-Pliocene simulations with NorESM-L – AGCM simulations

Z. Zhang[1,2,3] **and Q. Yan**[3]

[1]Bjerknes Centre for Climate Research, Allegaten 55, 5007, Bergen, Norway
[2]UNI Research, Allegaten 55, 5007, Bergen, Norway
[3]Nansen-Zhu International Research Center, Institute of Atmospheric Physics, Chinese Academy of Sciences, 100029, Beijing, China

Received: 18 April 2012 – Accepted: 26 April 2012 – Published: 9 May 2012

Correspondence to: Z. Zhang (zhongshi.zhang@bjerknes.uib.no)

Published by Copernicus Publications on behalf of the European Geosciences Union.

Abstract

In the Pliocene Model Intercomparison Project (PlioMIP), two sets of experiments are suggested. One includes a reference and a mid-Pliocene experiment run with atmosphere general circulation models (AGCM experiments, referred to as Experiments I), the other includes a pre-industrial and a mid-Pliocene experiment run with coupled ocean-atmosphere general circulation models (AOGCM experiments, referred to as Experiment II). In this paper, we describe the AGCM experiments with the atmosphere model in the low resolution version of the Norwegian Earth System Model (NorESM-L), and also assess the potential uncertainties in analyzing mid-Pliocene climate anomalies, due to choosing SST fields for the reference experiment. We carry out a mid-Pliocene experiment, a control experiment forced by the modern SST fields, and a pre-industrial experiment forced by the monthly SST fields from HadISST averaged between 1879 and 1900. Our experiments illustrate that the simulated mid-Pliocene global annual mean SAT is 17.1 °C. It is 2.5 °C warmer than the control experiment, but 2.7 °C warmer than the pre-industrial experiment. We find that the uncertainties in analyses of mid-Pliocene climate anomalies are small on a global scale, but still large on a regional scale. On the regional scale, these uncertainties should be noticed and assessed in future PlioMIP studies.

1 Introduction

The mid-Pliocene period, the most recent period in Earth's history, is thought to be an analog for the long term fate of the climate system in the coming future (e.g. Jansen et al., 2007; Dowsett et al., 2010; Meehl et al., 2007). It has been a focus for geological (e.g. Dowsett et al., 1992, 1994, 1996, 1999, 2009, 2010) and modeling (e.g. Chandler et al., 1994; Sloan et al., 1996; Haywood et al., 2000; Haywood and Valdes, 2004; Jiang et al., 2005; Yan et al., 2011) studies for more than one decade.

GMDD
5, 1203–1227, 2012

As the potential analog for the coming future, more attentions are paid to the mid-Pliocene warm period. The recent mid-Pliocene simulation (Lunt et al., 2009) and the reconstruction of *p*CO2 in the Pliocene (Pagani et al., 2009) indicate that climate sensitivity to the Earth system feedbacks is larger than the climate sensitivities to the fast feedbacks. The $\delta^{18}O$ record from the coral skeletons found in Philippines demonstrates that permanent El Niño conditions do not exist during the Pliocene warm period (Watanabe et al., 2011). New sensitivity analyses (Lunt et al., 2012) indicate that the elevated atmospheric CO_2 level is the main reason for the warm mid-Pliocene climate on a global scale. On a regional scale, the changes to ice sheets associated with orographic changes are the major reason for the stronger warming at high latitudes in the mid-Pliocene.

In order to better understand the dynamics behind the mid-Pliocene warm climate, and to further reduce gaps between simulations and reconstructions, the Pliocene Model Intercomparison Project (PlioMIP) is recently initiated (Haywood et al., 2010, 2011). Within the PlioMIP framework, an increasing number of mid-Pliocene experiments (e.g. Chan et al., 2011; Koenig et al., 2012; Yan et al., 2012; Zhang et al., 2012) are coming out. According to the PlioMIP experimental guidelines, two sets of experiments should be done, based on the PRISM (Pliocene Research, Interpretation and Synoptic Mapping) reconstructions (Dowsett et al., 2010). The first set includes a reference and a mid-Pliocene experiment run with atmosphere-only climate models (AGCM experiments, referred to as Experiments I). The second set includes a pre-industrial and a mid-Pliocene experiment run with coupled ocean-atmosphere climate models (AOGCM experiments, referred to as Experiment II).

Here, we describe the reference and mid-Pliocene experiments with the atmosphere component, Community Atmosphere Model version 4 (CAM4), in the low resolution version of the Norwegian Earth System Model (NorESM-L). The simulations with the coupled NorESM-L have been described by Zhang et al. (2012).

As the PlioMIP experimental guidelines suggest, the reference experiment is called pre-industrial experiment, but carried out based on local modern SST fields (Haywood

GMDD
5, 1203–1227, 2012

et al., 2010). However, modern SSTs are warmer than the pre-industrial. Whether the utilization of modern SSTs largely underestimates the climate anomalies between the mid-Pliocene and the pre-industrial is not assessed. Thus, in this paper, we also consider the potential influence of SST fields used in the reference experiment in analyses of the mid-Pliocene climate anomalies.

The experiments presented in the paper are contributions from the Bjerknes Centre for Climate Research (BCCR) and the Norwegian Climate Centre (NCC) to the PlioMIP Experiments I. Section 2 is the introduction to the CAM4 model. Different to Zhang et al. (2012), detailed boundary conditions, including SSTs, topography, vegetation and ice-sheet, are introduced in the Sect. 3. Section 4 shows the simulation results. Section 5 is discussion and summary.

2 Model description

The model used in this study is the spectral version of the Community Atmosphere Model CAM4 (Neale et al., 2010; Eaton, 2010), which is developed at the National Center for Atmospheric Research (NCAR). The resolution used for the model CAM4 is T31 in horizontal, approximately 3.75 degrees, and 26 levels in vertical. This model is exactly same as that used in the coupled simulations, and has been introduced by Zhang et al. (2012). However, two parameters, special for the NorESM-L, are listed here. The minimums relative humidity for low (cldfrc_rhminl) and for high (cldfrc_rhminh) stable clouds are resolution-dependent parameters. Due to the low resolution used here, the cldfrc_rhminl is set to 0.835, and the cldfrc_rhminh is set to 0.800. Other parameters are set to the default values for pre-industrial simulation with the CAM4. More introductions to the CAM4 can be found in the scientific description of CAM4 (Neale et al., 2010) and the user guide (Eaton, 2010). Detailed introduction to NorESM can be found in Alterskjær et al. (2011) and Zhang et al. (2012).

GMDD
5, 1203–1227, 2012

3 Boundary conditions and experimental designs

3.1 Sea surface temperature and sea ice

Following the PlioMIP experimental guidelines (Haywood et al., 2010), local modern SST and sea-ice fields should be used in the reference experiment. Our local modern SST and sea-ice fields (Fig. 1b, e) are created by Hurrell (2005), based on the Hadley Center SST anomalies with the Reynolds SST climatology. They represent the situation for 2000s, and are warmer than pre-industrial SSTs. Thus, we choose the monthly mean SSTs from 1870–1900 HadISST to create the pre-industrial SSTs. The pre-industrial SST fields (Fig. 1a, d) are created with the anomalies method suggested by the PlioMIP experimental guidelines (Haywood et al., 2010).

$$SST_{\text{pre-industial}} = HadISST_{1870–1900} - Modern_{Prism} + Modern_{Local}$$

In the pre-industrial SST fields, the sea-ice area is kept same as the local modern sea-ice area.

The mid-Pliocene SST and sea-ice fields (Fig. 1c and f) are also created with the anomalies method.

$$SST_{\text{mid-Pliocene}} = \text{mid-Pliocene } SST_{Prism} - Modern_{Prism} + Modern_{Local}$$

Sea ice area is set according to the rebuilt mid-Pliocene monthly SSTs. If the SST is higher than $-1.8\,^{\circ}C$, the sea ice coverage is set to 0.

3.2 Land-sea mask and topography

Following the PlioMIP experimental guidelines (Haywood et al., 2010), the reference experiment uses the local modern land-sea mask and topography conditions, since there are almost no changes between the modern and the pre-industrial land-sea mask and topography.

GMDD
5, 1203–1227, 2012

The mid-Pliocene land-sea mask used here is same as the local modern condition. It is the same mask as that used in the coupled simulation (Zhang et al., 2012). The mid-Pliocene topography is based on the topography file topo_v1.3 (Sohl et al., 2009), and created with the anomalies method (Fig. 2).

$$\mathrm{Top}_{\text{mid-Pliocene}} = \text{mid-Pliocene } \mathrm{Top}_{\mathrm{Prism}} - \mathrm{Modern}_{\mathrm{Prism}} + \mathrm{Modern}_{\mathrm{Local}}$$

Compared to the modern topography (Fig. 2b), large changes of topography appear on Greenland and the margin of Antarctic because of the retreat of ice-sheet. The Colorado and Andes mountains are higher in the mid-Pliocene topography condition.

3.3 Vegetation and ice-sheet

Following the PlioMIP experimental guidelines (Haywood et al., 2010), the pre-industrial experiment uses the vegetation and ice-sheet conditions (Fig. 3) for year 1850. The mid-Pliocene vegetation and ice sheet conditions are created based on the PRISM Pliocene land cover condition biom_veg_v1.2 (Hill et al., 2007; Salzmann et al., 2008). It is firstly changed to the LSM (Land System Model) vegetation types (https://wiki.ucar.edu/display/paleo/Biome4+conversion+to+LSM), and then converted to PFTs (Plant Function Types, http://www.cgd.ucar.edu/ccr/paleo/Notes/lsm2clm.txt). Compared to the pre-industrial vegetation, the percentage of bare land reduces, and the percentage of trees increases in the mid-Pliocene vegetation conditions (Fig. 3). Ice-sheet becomes smaller on Greenland and the margin of Antarctic. The vegetation and ice-sheet conditions are same as those used in the coupled simulations (Zhang et al., 2012).

3.4 Experimental designs

With the above conditions, we design three experiments here, the pre-industrial experiment, the control experiment, and the mid-Pliocene experiment (Table 1). The control experiment is the reference experiment suggested by the PlioMIP. These three

GMDD
5, 1203–1227, 2012

experiments are run for 50 yr. Time series of global mean surface air temperature are shown in Fig. 4a. In this paper, we calculate the climatological means from the last 20 yr of each simulation.

4 Results

4.1 Pre-industrial and control experiment

4.1.1 Surface air temperature

For the pre-industrial experiment, the global annual mean surface air temperature (SAT) is 14.4 °C. It is 0.2 °C colder than the global annual mean SAT 14.6 °C in the control experiment (Fig. 4a, Table 2). Both these two simulations are warmer than the pre-industrial temperature estimation, about 13.5 °C (Hansen et al., 2010), but close to the modern global mean SAT.

The simulated zonal mean SAT (Fig. 4b) is similar between the pre-industrial and the control experiment. It also agrees with the zonal mean ERA-interim temperature between 1979 and 2008 (Dee et al., 2011).

The simulated global annual SAT fields show the same pattern in the pre-industrial (Fig. 5a) and the control experiment (Fig. 5b). The highest SAT appears over the Western tropical Pacific Ocean and the Indian Ocean, where the annual mean SAT is higher than 28 °C. The coldest SAT occurs on the Antarctic, where the annual mean SAT is lower than −50 °C. Such pattern is in a good accordance with the ERA-interim annual temperature field (Fig. 5c, Dee et al., 2011).

4.1.2 Precipitation

In the pre-industrial experiment, the global annual mean precipitation is 2.9 mm day^{-1} (Table 2). It is same as the global annual mean precipitation in the control experiment. In these two experiments, highest zonal mean annual precipitation appears in the

GMDD
5, 1203–1227, 2012

Intertropical Convergence Zone (ITCZ), about 6.5 mm day^{-1} (Fig. 4c). In the two Poles, zonal mean annual precipitation is low, about 0.2 mm day^{-1}. The simulated zonal mean annual precipitation coincides with the zonal mean of observed precipitation from the Global Precipitation Climatology Project (GPCP; Adler et al., 2003) averaged over the period 1979–2008. The overall pattern and amount of simulated global precipitation fields are in good agreement with the observations (Fig. 5d–f).

4.2 Mid-Pliocene experiment

4.2.1 Surface air temperature

In the mid-Pliocene experiment, the global annual mean SAT is 17.1 °C (Table 1). It is 2.7 °C warmer than the pre-industrial experiment, and 2.5 °C warmer than the control experiment. Compared to the pre-industrial or the control experiment, stronger warming appears at high latitudes of the both hemispheres, whereas weak cooling occurs at tropics in the mid-Pliocene experiment (Fig. 6). Near equator, the zonal mean annual temperature increases only by 1 °C. At high latitudes of Southern Hemisphere, the zonal mean annual temperature increases by 11 °C. Largest warming appears near the North Pole, where the zonal mean annual temperature increases by 13 °C. Such changes, with stronger warming at high latitudes, follow the mid-Pliocene SST anomalies reconstructed by the PRISM (Dowsett et al., 2009), and also agree with other PlioMIP experiments (e.g. Chan et al., 2011; Koenig et al., 2012; Yan et al., 2012; Kamae and Ueda, 2012; Contoux et al., 2012).

Stronger warming at high latitudes also can be observed in the seasonal SAT anomalies fields, in particular in winter. In northern winter, zonal mean SAT over the Arctic in the mid-Pliocene experiment increases by 21 °C relative to the pre-industrial experiment, by 19 °C relative to the control experiment. In southern winter, zonal mean SAT on the margin of Antarctic in the mid-Pliocene experiment increases by 16 °C, relative to the pre-industrial or the control experiment.

GMDD
5, 1203–1227, 2012

4.2.2 Precipitation

In the mid-Pliocene experiment, the global annual mean precipitation is 3.0 mm day^{-1}. It is 0.1 mm day^{-1} larger than the global annual mean precipitation simulated in the pre-industrial and the control experiment.

The zonal mean precipitation shows that the mid-Pliocene annual precipitation decreases at tropics by 0.7 mm day^{-1} relative to the pre-industrial experiment, and by 0.6 mm day^{-1} relative to the control experiment. At tropics, the changes in precipitation have large regional variations. On the global precipitation anomalies map, larger annual precipitation increment (>3 mm day^{-1}) appears over the North Arabian Sea (on the coast of Middle East), tropical Africa, and the west coast of tropical South America. Larger annual precipitation deduction (< −3 mm day^{-1}) appears over Southern Indian, the South China Sea, the Bismarck Sea (on the north coast of the New Guinea island), and the tropical pacific on the coast of Central America.

At middle and high latitudes of both hemispheres, the zonal mean annual precipitation increases by about 0.5 mm day^{-1}. The changes of precipitation have less regional variations. The largest annual precipitation increment occurs over the Norwegian Sea, where the SSTs are remarkably increased in the PRISM mid-Pliocene reconstructions (Dowsett et al., 2009). The annual precipitation increases by 4 mm day^{-1} there.

The changes in global mean precipitation in the mid-Pliocene experiment are generally similar, relative to the pre-industrial experiment or the control experiment. However, apparent discrepancies exist in regional precipitation anomalies. For example over South Asia, the simulated mid-Pliocene annual precipitation decreases by 4 mm d^{-1} relative to the control experiment, but decreases by 6 mm d^{-1} referenced to the pre-industrial experiment.

GMDD
5, 1203–1227, 2012

5 Discussion and summary

As described in the above sections, the simulated temperature and precipitation in the pre-industrial and the control experiment agree with observations. The simulated mid-Pliocene climate is warmer than the pre-industrial and the control experiment, in particular at high latitudes. These simulations for basic pattern of mid-Pliocene warming agree well with our earlier coupled simulations (Zhang et al., 2012), and also other PlioMIP experiments (e.g. Chan et al., 2011; Koenig et al., 2012; Yan et al., 2012; Zhang et al., 2012; Kamae and Ueda, 2012; Contoux et al., 2012).

Analyses of mid-Pliocene climate anomalies depend on a reference experiment. In our study, if the control experiment is chosen to be the reference, as the PlioMIP experimental guidelines suggest, the mid-Pliocene global annual mean SAT increases by 2.5 °C. If the pre-industrial experiment is chosen to be the reference, the mid-Pliocene global annual mean SAT increase by 2.7 °C, which is 8 % larger than that referenced to the control experiment. This difference is not large, and to some extent can be neglected on a global scale.

However, on a regional scale, choosing reference experiment clearly influences the analyses of mid-Pliocene climate anomalies. For example, when the pre-industrial experiment is chosen to be the reference, the mid-Pliocene anomalies in zonal mean SAT is increased (decreased) by 30 % (55 %) at middle (low) latitudes, compared with the anomalies referenced to the control experiment (Fig. 8). In Indian, the simulated mid-Pliocene annual precipitation deduction is further enlarged by 50 %, when the pre-industrial experiment is chosen to be the reference.

The PlioMIP suggests to employ local modern SST fields in the reference experiment for Experiments I. The mid-Pliocene SST fields are created according to the anomalies method, in which the PRISM mid-Pliocene SST anomalies are added on the local modern SST fields. This experiment design is reasonable for considering climate sensitivity to the PRISM mid-Pliocene SST anomalies. It is also a common basis for the future comparisons of PlioMIP AGCM simulations.

GMDD
5, 1203–1227, 2012

However, it should be note, compared to the PlioMIP AOGCM simulations, the mid-Pliocene climate anomalies may be underestimated in the PlioMIP AGCM simulations. All PlioMIP AGCM simulations use modern SSTs in reference experiments, but all AOGCM experiments use pre-industrial simulations as reference experiments. We find this underestimation in our AGCM and AOGCM simulations (Zhang et al., 2012), and also the simulations carried by Chan et al. (2011), but not in the simulations carried by Kamae and Ueda (2012) and Contoux et al. (2012). This potential underestimation should be noticed and further assessed in the future PlioMIP synthesis and comparisons.

In summary, we describe the PlioMIP experiments I with the atmosphere model (CAM4) of the NorESM-L in this paper. According to the PlioMIP experimental guidelines, we carry out a mid-Pliocene experiment, and a control experiment forced by the local modern SST fields. We also carry out a pre-industrial experiment forced by the SST climatology from 1879–1900 HadISST, which is close to the pre-industrial condition. With these three AGCM experiments, we assess the potential uncertainties in analyzing mid-Pliocene climate anomalies.

Our experiments illustrate that the simulated mid-Pliocene global mean SAT is 17.1 °C. It is 2.7 °C warmer than the pre-industrial and 2.5 °C warmer than the control experiment. Choosing modern SSTs in the reference experiment only weakly underestimates mid-Pliocene climate anomalies on a global scale. However, on a regional scale, the potential uncertainties caused by choosing SSTs for the reference experiment should be noticed and assessed in future PlioMIP studies.

Acknowledgements. This study was jointly supported by the Earth System Modeling (ESM) project financed by Statoil, Norway, the National 973 Program of China (Grant No. 2010CB950102), and the National Natural Science Foundation of China (Grant No. 40902054). The NorESM development was supported by the Integrated Earth System Approach to Explore Natural Variability and Climate Sensitivity (EARTHCLIM) project, which is a nationally coordinated climate research project in Norway.

GMDD
5, 1203–1227, 2012

References

Adler, R. F., Huffman, G. J., Chang, A., Ferraro, R., Xie, P., Janowiak, J., Rudolf, B., Schneider, U., Curtis, S., Bolvin, D., Gruber, A., Susskind, J., and Arkin, P.: The version 2 Global Precipitation Climatology Project (GPCP) monthly precipitation analysis (1979-present), J. Hydrometeorol., 4, 1147–1167, 2003.

Alterskjær, K., Kristjánsson, J. E., and Seland, Ø.: Sensitivity to deliberate sea salt seeding of marine clouds – observations and model simulations, Atmos. Chem. Phys., 12, 2795–2807, doi:10.5194/acp-12-2795-2012, 2012.

Chan, W.-L., Abe-Ouchi, A., and Ohgaito, R.: Simulating the mid-Pliocene climate with the MIROC general circulation model: experimental design and initial results, Geosci. Model Dev., 4, 1035–1049, doi:10.5194/gmd-4-1035-2011, 2011.

Chandler, M., Rind, D., and Thompson, R.: Joint investigations of the middle Pliocene climate II: GISS GCM Northern Hemisphere results, Global Planet. Change, 9, 197–219, 1994.

Contoux, C., Ramstein, G., and Jost, A.: Modelling the mid-Pliocene Warm Period climate with the IPSL coupled model and its atmospheric component LMDZ4, Geosci. Model Dev. Discuss., 5, 515–548, doi:10.5194/gmdd-5-515-2012, 2012.

Dee, D. P., Uppala, S. M., Simmons, A. J., Berrisford, P., Poli, P., Kobayashi, S.,Andrae, U., Balmaseda, M. A., Balsamo, G., Bauer, P., Bechtold, P., Beljaars, A. C. M., van de Berg, L., Bidlot, J., Bormann, N., Delsol, C., Dragani, R., Fuentes, M., Geer, A. J., Haimberger, L., Healy, S. B., Hersbach, H., Hólm, E. V., Isaksen, L., Kållberg, P., Köhler, M., Matricardi, M., McNally, A. P., Monge-Sanz, B. M., Morcrette, J. J., Park, B. K., Peubey, C., de Rosnay, P., Tavolato, C., Thépaut, J. N., and Vitart, F.: The ERA-Interim reanalysis: configuration and performance of the data assimilation system, Q. J. Roy. Meteor. Soc., 137, 553–597, 2011.

Dowsett, H. J., Cronin, T. M., Poore, R. Z., Thompson, R. S., Whatley, R. C., and Haywood, A. M.: Micropaleontological evidence for increased meridional heat transport in the North Atlantic Ocean during the Pliocene, Science, 258, 1133–1135, 1992.

Dowsett, H. J., Thompson, R., Barron, J., Cronin, T., Fleming, F., Ishman, S., Poore, R., Willard, D., and Holtz, T.: Joint investigations of the middle Pliocene climate I: PRISM paleoenvironmental reconstructions, Global Planet. Change, 9, 169–195, 1994.

Dowsett, H. J., Barron, J., and Poore, R.: Middle Pliocene sea surface temperatures: a global reconstruction, Mar. Micropaleontol., 27, 13–25, 1996.

GMDD
5, 1203–1227, 2012

Dowsett, H. J., Barron, J. A., Poore, R. Z., Thompson, R. S., Cronin, T. M., Ishman, S. E., and Willard, D. A.: Middle Pliocene paleoenvironmental reconstruction: PRISM2, US Geol. Surv., Open File Rep., 99–535, 1999.

Dowsett, H. J., Robinson, M. M., and Foley, K. M.: Pliocene three-dimensional global ocean temperature reconstruction, Clim. Past, 5, 769–783, doi:10.5194/cp-5-769-2009, 2009.

Dowsett, H. J., Robinson, M. M., Haywood, A. M., Salzmann, U., Hill, D., Sohl, L., Chandler, M., Williams, M., Foley, K., and Stoll, D.: The PRISM3D paleoenvironmental reconstruction, Stratigraphy, 7, 123–139, 2010.

Eaton, B.: User's Guide to the Community Atmosphere Model CAM-4.0, http://www.cesm.ucar.edu/models/ccsm4.0/cam/docs/users_guide/ug.html (last access: December 2011), 2010.

Hansen, J., Ruedy, R., Sato, M., and Lo, K.: Global surface temperature change, Rev. Geophys., 48, RG4004, doi:10.1029/2010RG000345, 2010.

Haywood, A. M. and Valdes, P. J.: Modelling Pliocene warmth: contribution of atmosphere, oceans and cryosphere, Earth Planet. Sci. Lett., 218, 363–377, 2004.

Haywood, A. M., Valdes, P. J., and Sellwood, B. W.: Global scale palaeoclimate reconstruction of the middle Pliocene climate using the UKMO GCM: initial results, Global Planet. Change, 25, 239–256, 2000.

Haywood, A. M., Dowsett, H. J., Otto-Bliesner, B., Chandler, M. A., Dolan, A. M., Hill, D. J., Lunt, D. J., Robinson, M. M., Rosenbloom, N., Salzmann, U., and Sohl, L. E.: Pliocene Model Intercomparison Project (PlioMIP): experimental design and boundary conditions (Experiment 1), Geosci. Model Dev., 3, 227–242, doi:10.5194/gmd-3-227-2010, 2010.

Haywood, A. M., Dowsett, H. J., Robinson, M. M., Stoll, D. K., Dolan, A. M., Lunt, D. J., Otto-Bliesner, B., and Chandler, M. A.: Pliocene Model Intercomparison Project (PlioMIP): experimental design and boundary conditions (Experiment 2), Geosci. Model Dev., 4, 571–577, doi:10.5194/gmd-4-571-2011, 2011.

Hill, D. J., Haywood, A. M., Hindmarsh, R. C. A., and Valdes, P. J.: Characterising ice sheets during the mid Pliocene: evidence from data and models, in: Deep Time Perspectives on Climate Change: Marrying the Signal from Computer Models and Biological Proxies, edited by: Williams, M., Haywood, A. M., Gregory, F. J., and Schmidt, D. N., the Micropalaeontological Society, Special Publications, the Geological Society, London, 517–538, 2007.

Hurrell, J.: hurrell_sst_ifrac.1x1.050606.nc, available at: https://svn-ccsm-inputdata.cgd.ucar.edu/trunk/inputdata/ocn/docn7/SSTDATA/, last access: March 2011, 2005.

GMDD

5, 1203–1227, 2012

Jansen, E., Overpeck, J., Briffa, K. R., Duplessy, J.-C., Joos, F., Masson-Delmotte, V., Olago, D., Otto-Bliesner, B., Peltier, W. R., Rahmstorf, S., Ramesh, R., Raynaud, D., Rind, D., Solomina, O., Villalba, R., and Zhang, D.: Palaeoclimate, in: Climate Change 2007: The Physical Science Basis. Contribution of Working Group I to the Fourth Assessment Report of the Intergovernmental Panel on Climate Change, edited by: Solomon, S., Qin, D., Manning, M., Chen, Z., Marquis, M., Averyt, K. B., Tignor, M., and Miller, H. L., Cambridge University Press, Cambridge, UK and New York, NY, USA, 2007.

Jiang, D., Wang, H., Ding, Z., Lang, X., and Drange, H.: Modeling the middle Pliocene climate with a global atmospheric general circulation model, J. Geophys. Res., 110, D14107, doi:10.1029/2004JD005639, 2005.

Kamae, Y. and Ueda, H.: Mid-Pliocene global climate simulation with MRI-CGCM2.3: set-up and initial results of PlioMIP Experiments 1 and 2, Geosci. Model Dev. Discuss., 5, 383–423, doi:10.5194/gmdd-5-383-2012, 2012.

Koenig, S. J., DeConto, R. M., and Pollard, D.: Pliocene Model Intercomparison Project Experiment 1: implementation strategy and mid-Pliocene global climatology using GENESIS v3.0 GCM, Geosci. Model Dev., 5, 73–85, doi:10.5194/gmd-5-73-2012, 2012.

Lunt, D. J., Haywood, A. M., Foster, G., and Stone, E. J.: The Arctic cryosphere in the mid-pliocene and the future, Philos. T. R. Soc. A, 367, 49–67, 2009.

Lunt, D. J., Haywood A. M., Schmidt, G. A., Salzmann, U., Valdes, P. J., and Dowsett, H. J.: On the causes of mid-Pliocene warmth and polar amplification, Earth Planet. Sci. Lett., 321–322, 128–138, 2012.

Meehl, G. A., Stocker, T. F., Collins, W. D., Friedlingstein, P., Gaye, A. T., Gregory, J. M., Kitoh, A., Knutti, R., Murphy, J. M., Noda, A., Raper, S. C. B., Watterson, I. G., Weaver, A. J., and Zhao, Z. C.: Global climate projections, in: Climate Change 2007: The Physical Science Basis, Contribution of Working Group I to the Fourth Assessment Report of the Intergovernmental Panel on Climate Change, edited by: Solomon, S., Qin, D., Manning, M., Chen, Z., Marquis, M., Averyt, K. B., Tignor, M., and Miller, H. L., Cambridge University Press, Cambridge, UK and New York, NY, USA, 770–772, 2007.

Neale, R. B., Richter, J. H., Conley, A. J., Park, S., Lauritzen, P. H., Gettelman, A., Williamson, D. L., Rasch, P. J., Vavrus, S. J., Taylor, M. A., Collins, W. D., Zhang, M., and Lin, S.: Description of the NCAR Community Atmosphere Model (CAM 4.0), NCAR technical note, NCAR/TN-485+STR, 2010.

GMDD
5, 1203–1227, 2012

Pagani, M., Liu, Z., LaRiviera, J., and Ravelo, A. C.: High climate sensitivity to atmospheric carbon dioxide for the past 5 million years, Nat. Geosci., 3, 27–30, 2009.
Salzmann, U., Haywood, A. M., Lunt, D. J., Valdes, P. J., and Hill, D. J.: A new global biome reconstruction and data-model comparison for the Middle Pliocene, Global EcoL. Biogeogr., 17, 432–447, 2008.
Sloan, L. C., Crowley, T. J., and Pollard, D.: Modeling of middle Pliocene climate with the NCAR GENESIS general circulation model, Mar. Micropaleontol., 27, 51–61, 1996.
Sohl, L. E., Chandler, M. A., Schmunk, R. B., Mankoff, K., Jonas, J. A., Foley, K. M., and Dowsett, H. J.: PRISM3/GISS topographic reconstruction, US Geol. Surv. Data Series 419, 6 pp., 2009.
Vertenstein, M., Craig, T., Middleton, A., Feddema, D., and Fischer, C.: CESM1.0.3 User's Guide, available at: http://www.cesm.ucar.edu/models/cesm1.0/cesm/, last access: December 2011, 2010.
Watanabe, T., Suzuki, A., Minobe, S., Kawashima, T., Kameo, K., Minoshima, K., Aguilar, Y. M., Wani, R., Kawahata, H., Sowa, K., Nagai, T., and Kase, T.: Permanent El Niño during the Pliocene warm period not supported by coral evidence, Nature, 471, 209–211, 2011.
Yan, Q., Zhang, Z., Wang, H., Jiang, D., and Zheng, W.: Simulation of sea surface temperature changes in the Middle Pliocene warm period and comparison with reconstructions, Chinese Sci. Bull., 56, 890–899, 2011.
Yan, Q., Zhang, Z. S., Wang, H. J., Gao, Y. Q., and Zheng, W. P.: Set-up and preliminary results of mid-Pliocene climate simulations with CAM3.1, Geosci. Model Dev., 5, 289–297, doi:10.5194/gmd-5-289-2012, 2012.
Zhang, Z. S., Nisancioglu, K., Bentsen, M., Tjiputra, J., Bethke, I., Yan, Q., Risebrobakken, B., Andersson, C., and Jansen, E.: Pre-industrial and mid-Pliocene simulations with NorESM-L, Geosci. Model Dev., 5, 523–533, doi:10.5194/gmd-5-523-2012, 2012.

GMDD
5, 1203–1227, 2012

Table 1. Boundary conditions for the pre-industrial, the control and the mid-Pliocene experiment.

Conditions	Pre-Industrial	Control	Mid-Pliocene
Landsea mask	Local modern	Local modern	Local modern
Topography	Local modern	Local modern	Anomalies + local modern
SST	HadISST ano. + local modern	Local modern	PRISM SST ano. + local modern
CO_2	280 ppm	280 ppm	405 ppm
N_2O	270 ppb	270 ppb	270 ppb
CH_4	760 ppb	760 ppb	760 ppb
CFCs	0	0	0
Solar constant	1370 W m^{-2}	1370 W m^{-2}	1370 W m^{-2}
Vegetation	Local pre-industrial	Local pre-industrial	PRISM vegetation
Orbital parameters	Year 1950	Year 1950	Year 1950

GMDD
5, 1203–1227, 2012

Table 2. Global mean value for the pre-industrial, the control and the mid-Pliocene experiment.

Exp.	Pre-industrial	Control	Mid-Pliocene
Top energy balance	$-3.97\,W\,m^{-2}$	$-3.17\,W\,m^{-2}$	$0.39\,W\,m^{-2}$
Surface temperature	14.4 °C	14.6 °C	17.1 °C
Precipitation	$2.9\,mm\,d^{-1}$	$2.9\,mm\,d^{-1}$	$3.0\,mm\,d^{-1}$

GMDD
5, 1203–1227, 2012

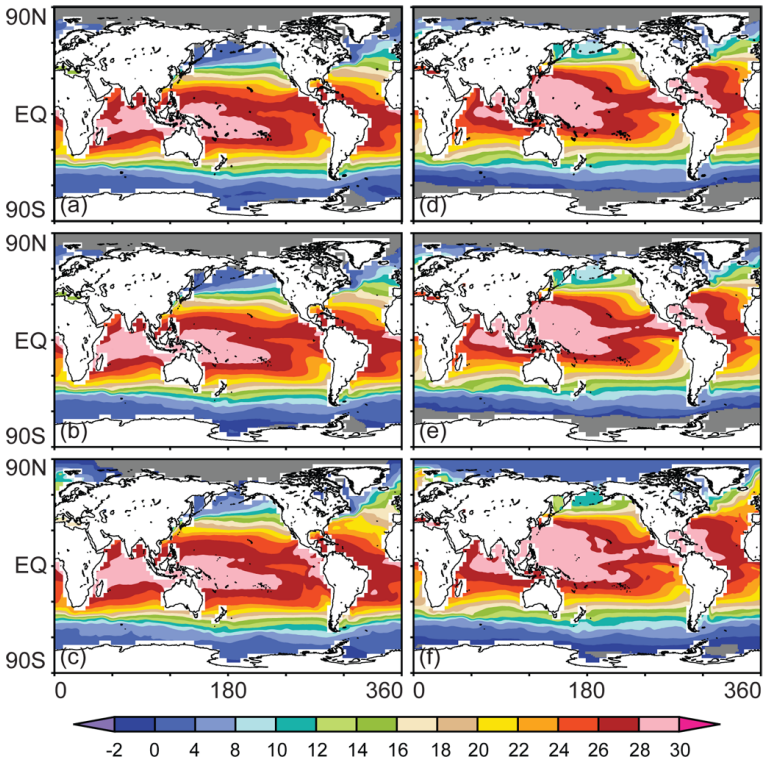

Fig. 1. SST (˚C) and sea-ice fields used in the experiments, left column for February, and right column for August. (**a** and **d**) for monthly mean HadISST between 1879–1900. (**b** and **e**) for local modern SST. (**c** and **f**) for mid-Pliocene SST. The gray shows the area of sea-ice.

GMDD
5, 1203–1227, 2012

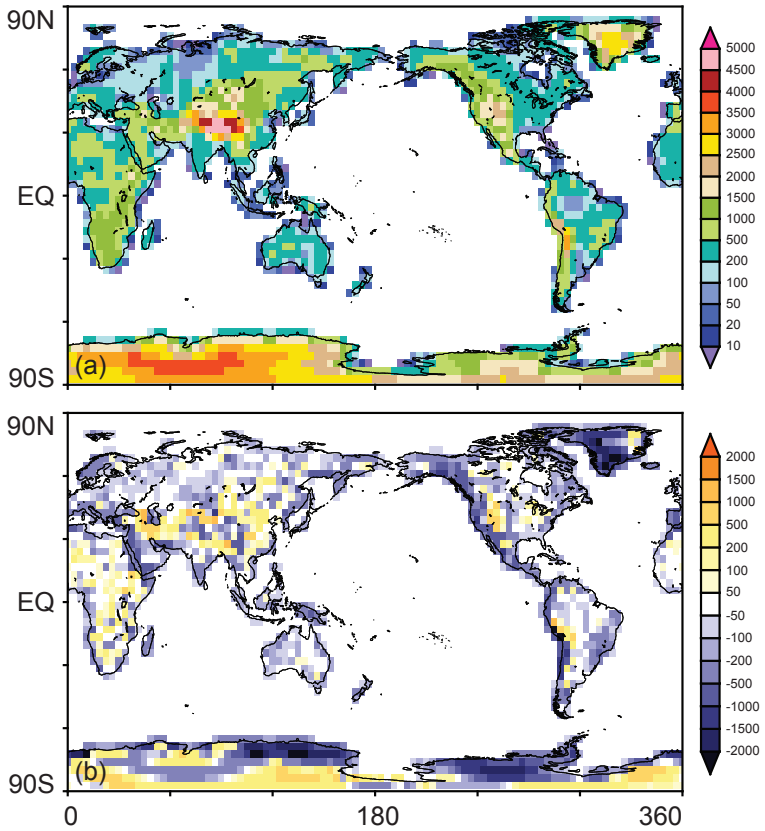

Fig. 2. Topography (m) conditions used in the experiments, **(a)** for local modern topography, **(b)** for the topography difference used to create the mid-Pliocene topography.

GMDD
5, 1203–1227, 2012

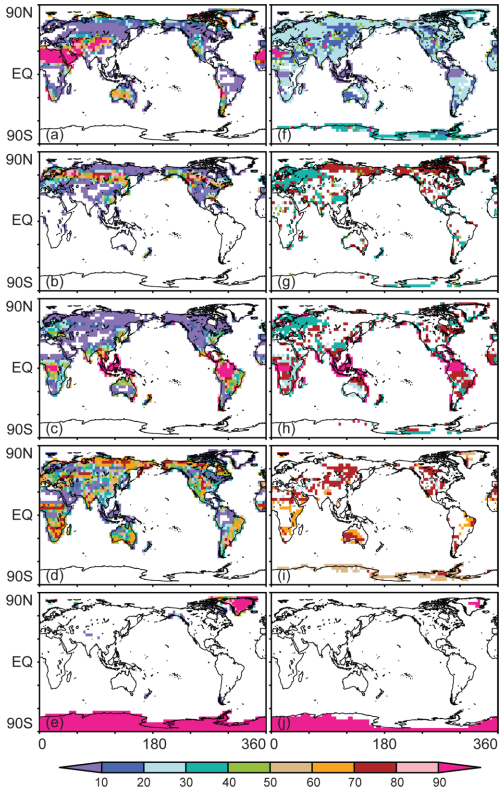

Fig. 3. Pre-industrial and mid-Pliocene land cover conditions (%), left column for the pre-industrial, right column for the mid-Pliocene. (**a** and **f**) for the percentage of bare land. (**b** and **g**) for the percentage of needleleaf trees, including needleleaf evergreen temperate tree, needleleaf evergreen boreal tree, and needleleaf deciduous boreal tree. (**c** and **h**) for the percentage of broadleaf trees, including broadleaf evergreen tropical tree, broadleaf evergreen temperate tree, broadleaf deciduous tropical tree, broadleaf deciduous temperate tree, and broadleaf deciduous boreal tree. (**d** and **i**) for the percentage of shrub and grass, including broadleaf evergreen temperate shrub, broadleaf deciduous temperate shrub, broadleaf deciduous boreal shrub, arctic C3 grass, cool C3 grass, warm C4 grass, and crop. (**e** and **j**) for the percentage of land ice.

GMDD
5, 1203–1227, 2012

Pre-industrial and mid-Pliocene AGCM simulation with NorESM-L

Z. Zhang and Q. Yan

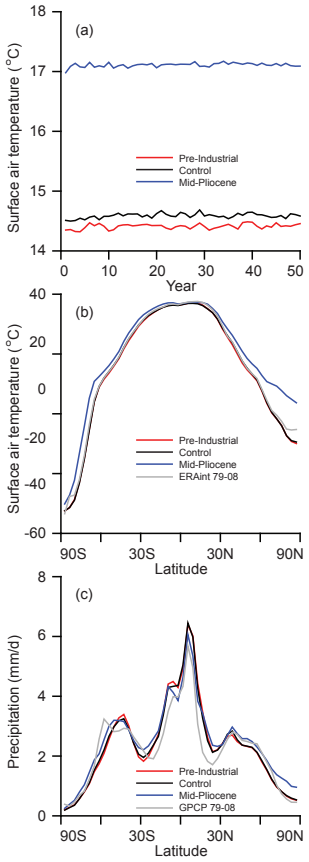

Fig. 4. (a) Time series of surface air temperature (°C) in the pre-industrial (red line), the control (black line), and the mid-Pliocene (blue line) experiment. **(b)** Simulated zonal mean annual surface air temperature (°C), with comparison to the ERA-interim temperature from 1979 to 2008. **(c)** Simulated zonal mean annual precipitation (mm d^{-1}), with comparison to the Global Precipitation Climatology Project (GPCP) 1979–2008 precipitation.

GMDD
5, 1203–1227, 2012

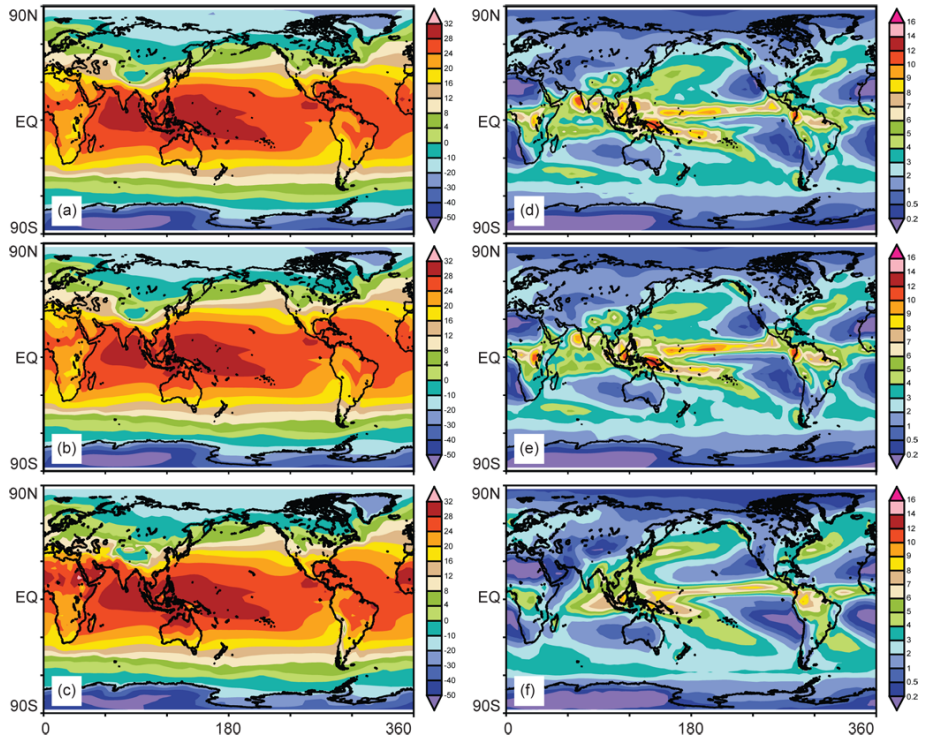

Fig. 5. Global annual surface air temperature (left column, °C) and precipitation (right column, mm d^{-1}) simulated in the pre-industrial (**a** and **d**), and the control (**b** and **e**) experiment, with comparison to the ERA-interim 1979–2008 surface air temperature **(c)** and GPCP 1979–2008 precipitation **(f)**.

GMDD
5, 1203–1227, 2012

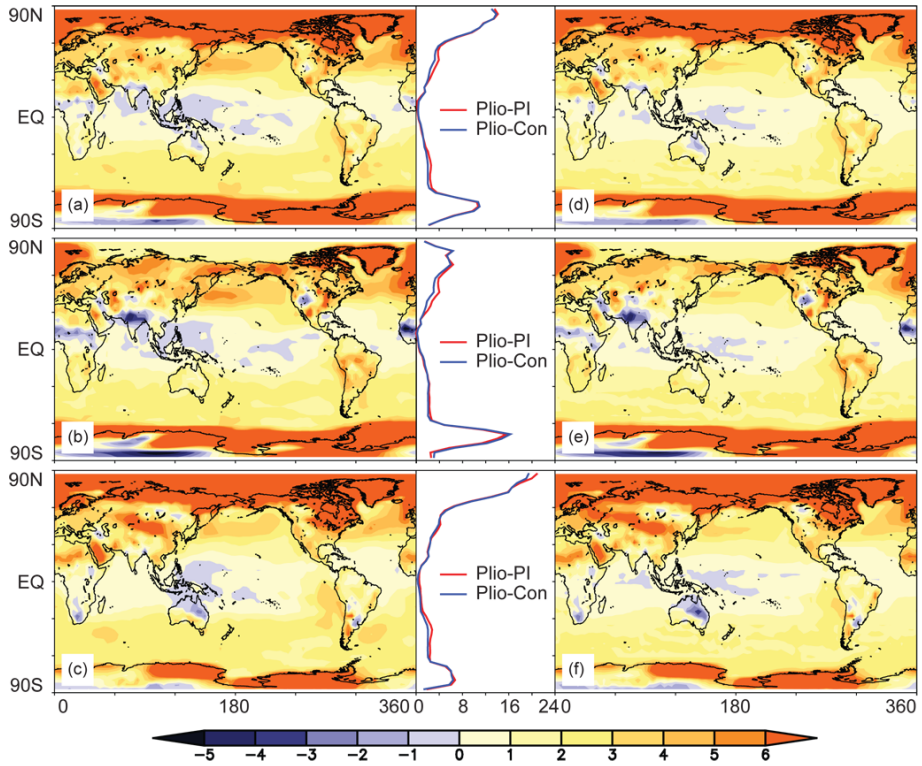

Fig. 6. Surface air temperature anomalies (˚C), left column for the anomalies between the mid-Pliocene and the pre-industrial experiment, right column for the anomalies between the mid-Pliocene and the control experiment. (**a** and **d**) for annual mean, (**b** and **e**) for boreal summer, and (**c** and **f**) for boreal winter. The bold lines in the middle show zonal mean values for these anomalies.

GMDD
5, 1203–1227, 2012

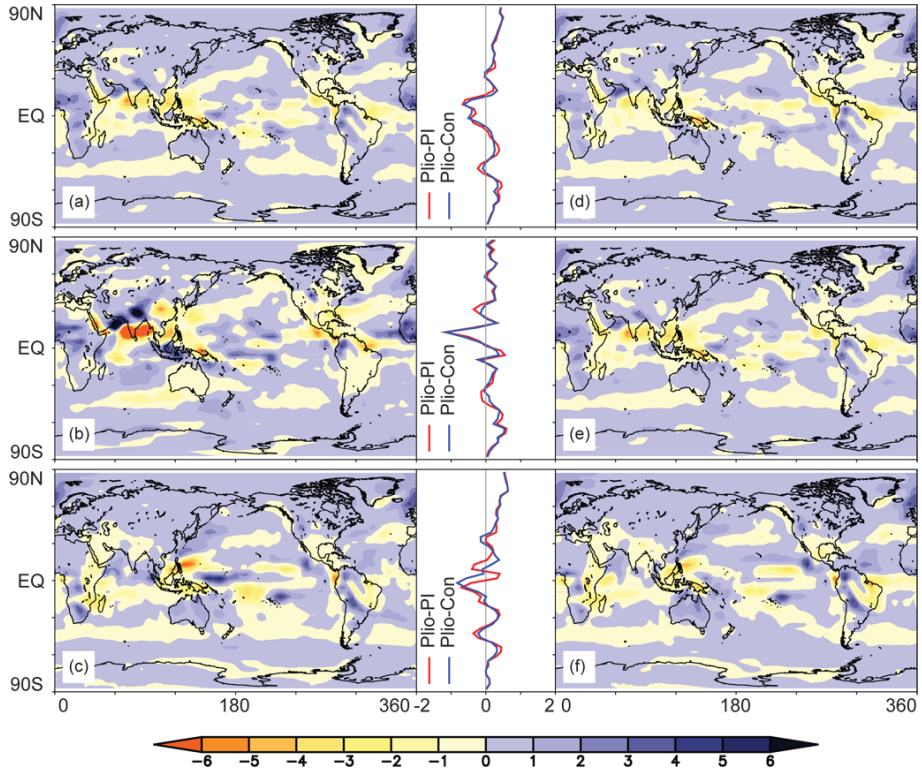

Fig. 7. Precipitation anomalies (mm d^{-1}), left column for the anomalies between the mid-Pliocene and the pre-industrial experiment, right column for the anomalies between the mid-Pliocene and the control experiment. (**a** and **d**) for annual mean, (**b** and **e**) for boreal summer, and (**c** and **f**) for boreal winter. The bold lines in the middle show zonal mean values.

GMDD
5, 1203–1227, 2012

Pre-industrial and mid-Pliocene AGCM simulation with NorESM-L

Z. Zhang and Q. Yan

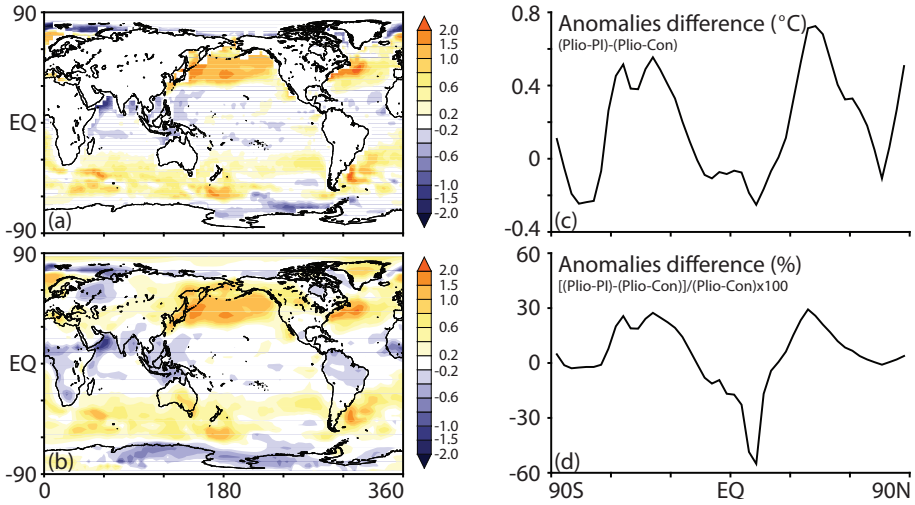

Fig. 8. Uncertainties in mid-Pliocene SAT anomolies, due to choosing SST fields in the reference experiment. **(a)** Differences in annual mean SST between the local modern and the 1879–1900 HadISST. **(b)** Differences between mid-Pliocene SAT anomalies relative to the pre-industrial and relative to the control experiment, Fig. 6a minus Fig. 6d. **(c)** The zonal mean for **(b)**. **(d)** The percentage of the zonal difference in **(c)**, relative to the zonal mean SAT anomalies between the mid-Pliocene and the control experiment.

GMDD
5, 1203–1227, 2012